

## NMR Structure Determination of Saccharose and Raffinose by Means of Homo- and Heteronuclear Dipolar Couplings

by Heike Neubauer, Jens Meiler, Wolfgang Peti, and Christian Griesinger\*

Max Planck Institut für Biophysikalische Chemie, Am Fassberg 11, D-37077 Göttingen, Germany

---

Residual dipolar couplings have dramatically improved the accuracy and precision of high-resolution NMR structures during the last years. This was first demonstrated for proteins. In this article, we describe, with raffinose and saccharose as examples, that dipolar couplings improve the precision of structures of carbohydrates for which usually very few structural parameters are available. The relative orientation as well as the dynamics of the monosaccharide moieties with respect to each other can be determined with the help of  $^{13}\text{C},^1\text{H}$  and  $^1\text{H},^1\text{H}$  dipolar couplings, which can easily be measured. Significant differences between the solution and the X-ray crystal structure exist. These results indicate that residual dipolar-coupling data may provide a more complete and dynamic model of carbohydrates in particular, and small molecules in general.

---

**1. Introduction.** – The use of residual dipolar couplings [1][2] observed when proteins are subjected to an orienting environment has already had considerable impact on the precision of protein-structure determination by means of high-resolution NMR spectroscopy of liquids [3–5]. In uniformly  $^{13}\text{C},^{15}\text{N}$ -labeled proteins, a large number of dipolar couplings is experimentally accessible. These dipolar couplings can be measured for internuclear vectors such as  $\text{NH}$ ,  $\text{NC}_\alpha$ ,  $\text{C}_\alpha\text{C}'$ ,  $\text{NC}'$ , and  $\text{H}_\alpha\text{C}_\alpha$ , which are isotropically distributed for many globular proteins [6–8]. Heteronuclear dipolar couplings have also been utilized to derive structures of small ligands bound to proteins [9–11]. For small molecules, few NOEs and scalar coupling constants can be measured that define, for example, the conformation across the glycosidic bonds in oligosaccharides [12]. However, there are several major difficulties that need to be considered in oligosaccharides. First, in contrast to proteins, fewer C,H dipolar couplings across a single bond can be measured. Second, the distribution of C,H bond vectors is not isotropic due to the geometry of the pyranose rings [13–17]. As a consequence, an alignment tensor cannot easily be derived for oligosaccharides oriented in bicelles [18]. Third, it is known that oligosaccharides are often flexible around the glycosidic bonds that connect the different sugar moieties. Therefore, different alignment tensors can be observed for the monosaccharides constituting the oligosaccharide. However, investigations of oligosaccharides published so far rely on C,H dipolar couplings from which individual alignment tensors for the monosaccharides cannot be derived. Therefore, in these studies, it is assumed without proof that the alignment tensor is the same for all monosaccharide moieties [13][15–17].

To overcome the potential problems, we increased the number of experimental dipolar couplings by measuring C,H dipolar couplings but also including H,H dipolar couplings. For this study, residual dipolar couplings were recorded for saccharose (=  $\beta$ -D-fructofuranosyl- $\alpha$ -D-glucopyranoside) and raffinose (=  $\beta$ -D-fructofuranosyl *O*- $\alpha$ -D-

galactopyranosyl-(1 → 6)- $\alpha$ -D-glucopyranoside). With the additional homonuclear residual dipolar couplings, it was possible to obtain an alignment tensor for each monosaccharide. This enables the evaluation of the mobility of each of the monosaccharides.

**2. Results and Discussion.** – 2.1 *Measurement of Homo- and Heteronuclear Dipolar Couplings.* Since heteronuclear and homonuclear dipolar couplings are observed on top of scalar couplings, the general strategy is to record couplings on a sample of the oligosaccharide with and without alignment. The methods used are the HSQC [19] without decoupling in the  $^{13}\text{C}$  dimension for measurement of the C,H couplings, the SPITZE-HSQC [20] for the measurement of the C,H and H,H dipolar couplings of  $\text{CH}_2$  groups, and E.COSY [21–23], for the first time, for the measurement of the H,H dipolar couplings in carbohydrates. All these experiments provide residual dipolar coupling constants with the sign and size [24][25] required to translate them in the least ambiguous way into orientational information. As for C,H-HSQC and the SPITZE HSQC residual dipolar-coupling measurement have been described in [19][20], we subsequently focus on the extraction of H,H dipolar couplings from E.COSY spectra. In the discussion below, referring to a coupling constant corresponds to the superposition of the scalar ( $J$ ) and the dipolar coupling ( $D$ ). Consider a system consisting of three mutually coupled spins A, B, and C. From an E.COSY cross-peak between spins A and B we can extract the C,B coupling constant from the  $\omega_2$  component of the displacement vector due to C, provided the sum of the A,C coupling is resolved in  $\omega_1$ . The size and the sign of the C,B coupling constant can be determined provided the sign of the associated coupling constant between A and C is known [23]. Since the sign of the coupling constant is known only if the scalar couplings are larger than the dipolar couplings, the alignment should be rather weak.

Three types of E.COSY cross-peaks can be observed in anisotropic solutions. First, we see cross-peaks between scalar coupled protons. An example for this case is the extraction of dipolar couplings from the cross-peaks between the vicinal protons H3,H2 and H3,H4 of glucose, which is part of raffinose, in the isotropic (*Fig. 1, a*) and the anisotropic medium (*Fig. 1, b*). The passive spins are H1 and H4 in the H2/H3 cross-peak, and H2 and H5 in the H4/H3 cross-peak. While in the isotropic phase the  $^4J(\text{H,H})$  couplings are usually close to zero, the H3,H2 cross-peak in the oriented phase shows a sizeable  $(D + J)(\text{H2,H4}) = -1.74$  Hz coupling, as does the H3/H4 cross-peak. The sign of the coupling is derived from the fact that the vector lies in the second or fourth quadrant of the  $\omega_2, \omega_1$  coordinate system, which means that the sign is opposite to the positive sign of the associated  $(D + J)(\text{H3,H4})$  or  $(D + J)(\text{H3,H2})$  coupling. This procedure provides dipolar couplings between protons separated by four bonds from the cross-peaks between vicinal protons in the oligosaccharide.

The second case are cross-peaks when the active coupling is due to residual dipolar couplings, and which, thus, are not observed in isotropic media. For example, the fructose H6'/H4 cross-peak (*Fig. 2*) originates from the  $D(\text{H6}',\text{H4})$  coupling alone. This cross-peak contains three displacement vectors due to couplings of H6, H5, and H3, with H6' and H4. They can be assigned due to the fact that H6 shows the largest displacement in  $\omega_1$ , H3 shows no displacement in  $\omega_2$ , and H5 causes a displacement in both  $\omega_1$  and  $\omega_2$ . Again, sign and size of the coupling constants can be derived.

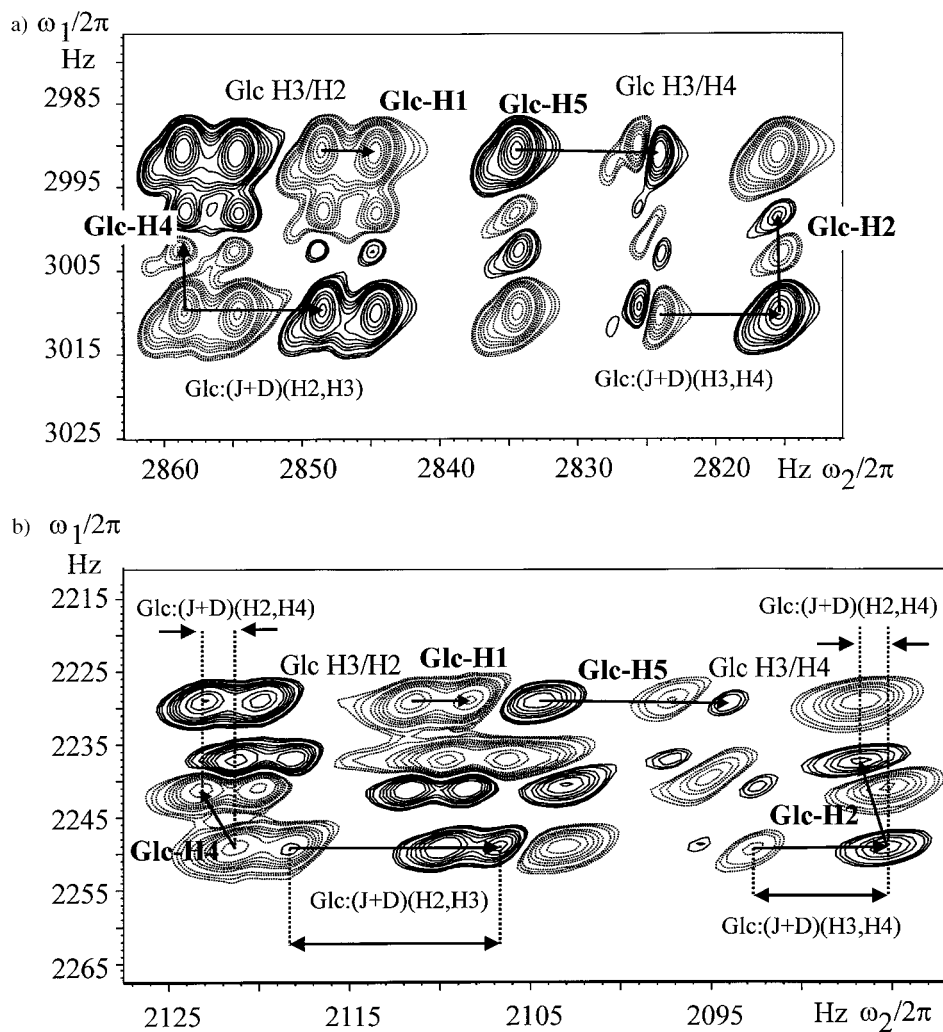


Fig. 1. The H3/H2 and H3/H4 cross-peaks of glucose in raffinose recorded in a) isotropic solution and in b) CHAPSO/DMPC (1/3.5; 7.5%). Positive contours are full, negative contours are plotted in dashed lines. The passive spins and the respective displacement vectors are given in bold. Measuring the displacement preferably in  $\omega_2$  yields size and sign of the coupling constants of interest. The displacement vectors for Glc-H2 and Glc-H4 lack an  $\omega_2$  component in isotropic phase, whereas they reflect the pure dipolar Glc (H2,H4) coupling in the anisotropic medium.

Finally in the last case, the E.COSY spectrum can also contain cross-peaks that do not show an E.COSY pattern, because one of the two possible couplings between spins A and C, or B and C is zero. This situation is encountered for protons that belong to different monosaccharides in the trisaccharide. Then, only the extraction of the active coupling is possible, for which the sign cannot be determined. The extraction is done according to the DISCO [26–28] method by comparison with other cross-peaks. This is

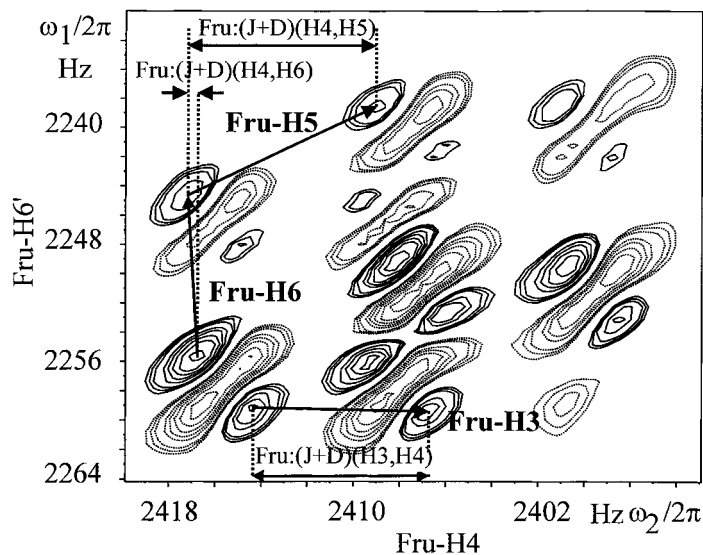


Fig. 2. H6/H4 Cross-peak of fructose in raffinose recorded in CHAPSO/DMPC (1/3.5; 7.5%). Positive and negative contours marked as in Fig. 1. The passive spins are H6, H5, and H3. They can be easily distinguished due to the different vector components in  $\omega_1$  and  $\omega_2$ . Size and sign of the coupling constants of interest are measured from the  $\omega_2$  component of the displacement vectors and reported in Table 2.

shown using the Gal-H1/Glc-H6 cross-peak that is compared with the Glc-H6/H6 cross-peak in Fig. 3. The dipolar as well as the scalar coupling constants that could be extracted from raffinose and saccharose are compiled in Tables 1 and 2 and 6 and 7, respectively.

**2.2. Materials and Methods.** Raffinose and saccharose were purchased from Fluka (Buchs, Switzerland) and used without further purification. Samples of 20 mM raffinose or saccharose in 500  $\mu$ l D<sub>2</sub>O in regular thin-wall NMR tubes were used. For the alignment, bicelles were formed from CHAPSO/DMPC (1/3.5, 7.5%) (CHAPSO/DMPC purchased from Sigma (St. Louis, MO, USA); SDS purchased from Merck (Darmstadt, Germany), and used without further purification) [29–31]. For saccharose, dipolar couplings were measured with CHAPSO/DMPC (1/3.5, 7.5%). For raffinose, two sets of dipolar couplings in CHAPSO/DMPC (1/3.5, 7.5%) and CHAPSO/DMPC/SDS (1/3.5/0.2, 7.5%) were measured. Since small carbohydrates have no charge, the difference between the two data sets is small. Therefore, all calculations have been performed with the CHAPSO/DMPC data set. Interestingly, the CHAPSO/DLPC bicelles did not align the carbohydrates very well. This is different compared with proteins [20][30][32]. All experiments were performed either on a Bruker DRX-600 or Bruker DRX-800 spectrometer (Bruker AG, Rheinstetten, Germany) equipped with TXI HCN  $z$ -grad probes. The temperature for all measurements was set to 308 K, except for the NOESY spectra (280 K). All spectra were processed with XWINNMR 2.6 (Bruker AG, Karlsruhe, Germany).

For all experiments, the proton carrier was set to 4.7 ppm (HDO resonance) and for carbons to 82 ppm. The recycle delay was set between 2 and 5 s according to inversion

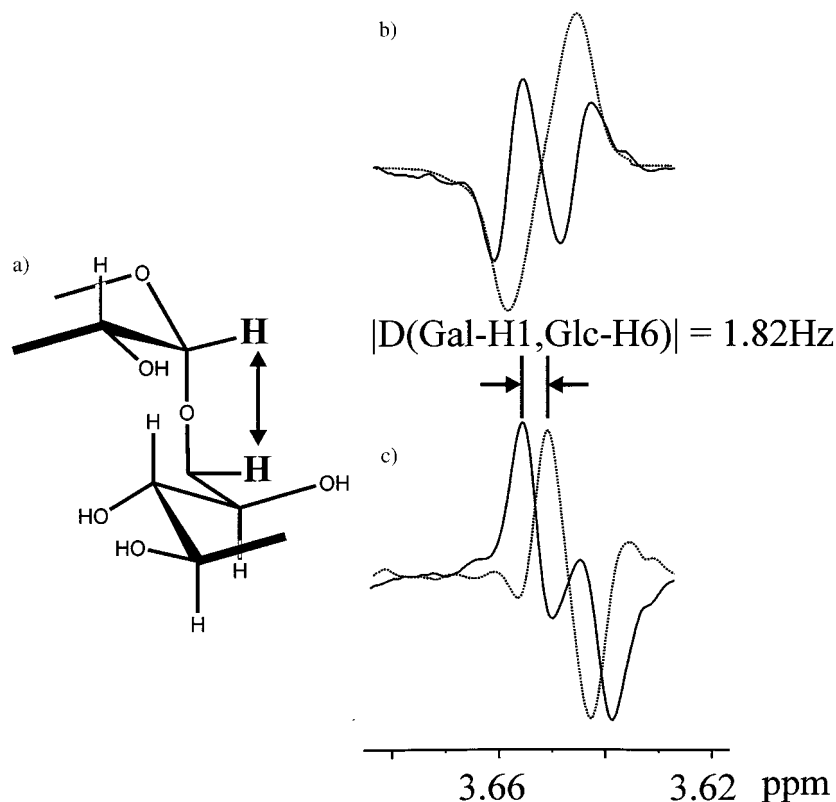


Fig. 3. a) Schematic picture of the galactose and glucose linkage in raffinose. b) Solid line: trace obtained by summation along  $\omega_1$  over the Gal-H1, Glc-H6 cross-peak that is purely caused by the dipolar coupling. Broken line: trace obtained in the same way from the Glc-H6', H6 cross-peak. c) DISCO Procedure applied to the two traces of b, taking the sum (solid line) and difference (broken line). The difference in the line positions of the two peaks provides the absolute value of the desired (Gal-H1, Glc-H6) dipolar coupling constant, but not its sign.

recovery  $T_1$  experiments. Coupled HSQC spectra were recorded with  $2\text{k} \times 4\text{k}$  and zero-filled to establish 0.4-Hz resolution for the exact measurement of the  $^1J(\text{C}, \text{H})$  couplings (measurement time 6 h). The SPITZE HSQC was recorded as described by *Carlomagno et al.* (measurement time 8 h for each experiment, zero-filled to obtain a resolution of 0.3 Hz in  $\omega_2$ .) [20]. H,H Dipolar couplings were recorded according to the P.E.COSY [22][33] method.  $4\text{k} \times 1\text{k}$  Data points (measurement time 10 h) were recorded in the experiment and then zero-filled to  $8\text{k} \times 4\text{k}$  to obtain the desired resolution of 0.2 Hz. 2D NOESY Spectra were recorded at different mixing times to obtain distance restraints (measurement temperature 280 K to increase  $\tau_c$ ). Build-up curves [34] were measured at 800 MHz from 200 to 1100 ms (measurement time 11 h). For raffinose, the optimal mixing time is 500 ms ( $4\text{k} \times 1\text{k}$  and zero-filled to  $16\text{k} \times 4\text{k}$ ). To suppress zero-quantum peaks, the NOESY spectra were recorded with an incremented mixing time and the 500-ms NOESY with a random variation of the mixing time [34][35].

*Structure Refinement.* The two carbohydrate structures were refined in order to determine the relative orientation of the monosaccharides using the X-Plor program [36] together with an optimized force field for saccharides [37], and NOEs and dipolar-coupling restraints. A standard simulated annealing protocol was used together with dipolar coupling restraints implemented as angle restraints [38]. NOE Distances were translated into a standard X-Plor potential. For calculating the angle restraints from the dipolar couplings, as well as for fitting the structures to the experimental data and for determining the alignment tensor size and orientation, the program *DipoCoup* [39] was used. In every experiment, 100 structures were generated and those 10 with the lowest energies were further analyzed.

*Determination of the Alignment Tensor for Each Monosaccharide.* The determination of the tensor size according to *Clore et al.* [18] cannot be performed due to the relatively low number of dipolar couplings available per monosaccharide. For an individual structural unit, for instance, one of the monosaccharides, one needs at least five linearly independent equations to obtain the alignment tensor [25][39][40]. However, for glucose and galactose there are only two linearly independent C,H orientations, which lead to only two linearly independent equations. Thus, the tensor determination for each monosaccharide unit from C,H couplings alone is impossible. Nevertheless, including H,H dipolar couplings, this number can be increased well over five independent equations. To obtain insight into the error propagation of dipolar couplings with respect to the alignment tensor, we did the following test: the lowest-energy structure of raffinose (see below) and the firm experimental dipolar couplings ('firm' dipolar couplings are those that are used for structure calculation) were used, and the alignment tensor was individually fitted to the monosaccharides. For galactose, we obtained:  $D_{ax} = -3.09 \pm 0.26$  Hz,  $R = 0.45 \pm 0.19$ , for glucose:  $D_{ax} = -5.60 \pm 0.73$  Hz,  $R = 0.56 \pm 0.09$ , and for fructose:  $D_{ax} = 7.20 \pm 0.93$  Hz,  $R = 0.60 \pm 0.08$  ( $D_{ax}$  is the value for the axial component and  $R$  for the rhombicity of the alignment tensor [2][39]). The errors have been derived by randomly adding or subtracting an experimental uncertainty of  $\pm 0.2$  Hz to or from the experimental H,H dipolar couplings and  $\pm 0.4$  Hz to or from the experimental C,H dipolar couplings. For the structure calculations, an error of *ca.*  $\pm 20\%$  for the axial component and the rhombicity of the tensor was derived. Due to the uncertainty of the alignment tensor, a grid search over this region was performed. The starting size of the tensor was taken from the experimental dipolar couplings and the neutron diffraction or X-ray structure as a model for the solution structure. The step size of the grid search was chosen to contain all possible and structural meaningful values for the axial component and the rhombicity of the alignment tensor. After selection of ten structures with the lowest  $Q$  values ( $Q$ -value filtration), the alignment tensor was back-calculated from those structures by *Moore-Penrose* inversion [39] to check for self-consistency of the alignment tensor. Cross validation on the basis of unused dipolar-coupling data was carried out for those structures that had a self-consistent alignment tensor.

*2.3. Structure Calculation of Raffinose.* Measured scalar and dipolar couplings are given in *Tables 1* and *2*. Not all of them were used for the structure calculations. Since the protocol does not allow ensemble calculations, only one conformation could be calculated in each run. Therefore, couplings that are subject to conformational averaging are excluded from the fitting for the determination of the alignment tensor as

well as from the structure calculation. The same holds for protons with overlapping chemical shifts. The dipolar couplings of the glucose C6 H<sub>2</sub> group could be used for the structure calculation, because the population of the C5,C6 torsion angle is mainly  $g^-$  ( $g^-$ :75%,  $g^+$ :25%,  $t$ :0%) as derived from  $J$ -coupling analysis [42]. The stereochemical assignment of the diastereotopic protons could be accomplished on the basis of the Glu-H6,H4 NOE ( $\delta(\text{C6 H}^{pro-R}) = 4.08$  ppm,  $\delta(\text{C6 H}^{pro-S}) = 3.74$  ppm). In contrast, the fructose C6 H<sub>2</sub> group adopts two conformations, 66% of  $g^+$  and 32% of  $g^-$  ( $\delta(\text{C6 H}^{pro-R}) = 3.82$  ppm,  $\delta(\text{C6 H}^{pro-S}) = 3.88$  ppm) and could, therefore, not be used in the structure-calculation protocol. The two protons at the galactose C6 are degenerate as are the protons at fructose C1. All the excluded couplings are marked with a star in *Table 1* and are used for cross validation. We call the other dipolar couplings firm experimental couplings and use them for the derivation of the monosaccharide alignment tensors as well as for the structure determination.

Table 1. *Dipolar Couplings Determined for Raffinose in CHAPSO/DMPC (1/3.5; 7.5%)*. The three dipolar couplings with undefined sign were extracted according to the described DISCO procedure. The couplings not marked by stars are the ‘firm’ couplings as introduced in the text.

	$D(\text{C,H})$ [Hz]		$D(\text{H,H})$ [Hz]
Gal-C1/H1	2.60	Gal-H1/H2	-1.10
Gal-C2/H2	-3.64	Gal-H2/H3	0.23
Gal-C3/H3	-3.42	Gal-H3/H4	0.20
Gal-C4/H4	3.38	Gal-H4/H5	-0.99
Gal-C5/H5	-3.94	Gal-H3/H5	$\pm 1.78$
*Gal-C6/H6;H6'	-2.34	Glc-H1/H2	-0.61
Glc-C1/H1	5.28	Glc-H2/H3	1.70
Glc-C2/H2	2.73	Glc-H3/H4	-1.00
Glc-C3/H3	2.34	Glc-H4/H5	-0.30
Glc-C4/H4	1.52	*Glc-H5/H6	-2.50
Glc-C5/H5	3.29	Glc-H6/H6'	2.90
Glc-C6/H6	3.90	Glc-H2/H4	-1.74
Glc-C6/H6'	1.90	Glc-H3/H5	0.00
*Fru-C1/H1;H1'	4.55	Fru-H3/H4	-2.48
Fru-C3/H3	-6.54	Fru-H4/H5	0.69
Fru-C4/H4	-4.76	*Fru-H5/H6	-1.20
Fru-C5/H5	-2.60	*Fru-H5/H6'	-1.24
*Fru-C6/H6	1.80	*Fru-H6/H6'	1.70
*Fru-C6/H6'	-2.00	Fru-H3/H5	1.01
*Gal-H1/Glc-H6'	$\pm 1.82$	*Fru-H4/H6	0.50
*Gal-H5/Glc-H4	$\pm 1.56$	*Fru-H4/H6'	0.70
*Gal-H1/Glc-H6	$\pm 1.45$		

Alignment tensors for each monosaccharide from firm heteronuclear  $D(\text{C,H})$  dipolar couplings and the combination of firm heteronuclear and homonuclear dipolar  $D(\text{C,H}) + D(\text{H,H})$  dipolar couplings were extracted by fitting these firm dipolar-coupling constants against the X-ray structure of raffinose [42] individually for each monosaccharide and for the whole structure [39]. Using the firm dipolar couplings, we find the following tensor sizes for the monosaccharides from the CHAPSO/DMPC data: galactose:  $D_{\text{ax}} = -3.11$  Hz,  $R = 0.35$ , glucose:  $D_{\text{ax}} = -5.60$  Hz,  $R = 0.57$ , fructose:  $D_{\text{ax}} = 7.01$  Hz,  $R = 0.56$  (*Table 3*). The tensor sizes for glucose and fructose are similar

Table 2. *Scalar Couplings Determined for Raffinose in Isotropic Solution.* Also NOE distances measured as described in the text of the paper are listed. The Glc-H1/H2 cross-peak was used as reference peak. The star indicates the sum of two couplings.

	$^1J(\text{C,H})$ [Hz]		$J(\text{H,H})$ [Hz]		NOE [ $\text{\AA}$ ]
Gal-C1/H1	170.6	Gal-H1/H2	3.93	Gal-H1/Glc-H6'	2.52
Gal-C2/H2	146.3	Gal-H2/H3	10.30	Gal-H1/Glc-H6	2.78
Gal-C3/H3	145.5	Gal-H3/H4	3.45	Glc-H1/H2*	2.41
Gal-C4/H4	146.8	Gal-H4/H5	1.20	Glc-H4/H6	2.62
Gal-C5/H5	142.9	Glc-H1/H2	3.96	Gal-H5/Glc-H4	3.05
Gal-C6/H6;H6'	287.9*	Glc-H2/H3	9.89	Glc-H4/H6	3.33
Glc-C1/H1	169.7	Glc-H3/H4	8.76	Glc-H1/Frau-H1	2.44
Glc-C2/H2	144.6	Glc-H4/H5	10.40	Fru-H4/H6'	2.71
Glc-C3/H3	145.0	Glc-H5/H6	3.96	Fru-H4/H6	2.99
Glc-C4/H4	145.9	Glc-H6/H6'	– 10.90	Gal-H1/H2	2.37
Glc-C5/H5	145.5	Fru-H3/H4	8.79	Gal-H3/H5	2.73
Glc-C6/H6	145.5	Fru-H4/H5	8.45	Glc-H3/H5	2.60
Glc-C6/H6'	144.3	Fru-H5/H6	3.00		
Fru-C1/H1;H1'	290.1*	Fru-H5/H6'	7.32		
Fru-C3/H3	149.8	Fru-H6/H6'	– 12.21		
Fru-C4/H4	144.2	Glc-H5/H6'	2.26		
Fru-C5/H5	144.2				
Fru-C6/H6	143.6				
Fru-C6/H6'	142.6				

Table 3. *Tensor Sizes for Raffinose in CHAPSO/DMPC (1/3.5; 7.5%).* The average alignment tensor of the ten structures with lowest energy from 100 XPLOR calculations is given. The values for the two calculated data sets with the lowest  $Q$  values, and the most self-consistent  $D_{\text{ax}}$  and  $R$  values are shown. The galactose, glucose, and fructose structures are derived from the two best data sets of the solution structure of raffinose. The items indicated with § refer to the neutron-diffraction structure of saccharose, the item indicated with § refers to the X-ray structure of raffinose. The tensor size and rhombicity using only heteronuclear dipolar couplings ( $D(\text{C,H})$  in Table 3) are not sufficient to determine the alignment tensor for each of the monosaccharides due to too few linearly independent orientations.

	$D_{\text{ax}}$ [Hz]	$R$	$Q$
§Gal: $D(\text{C,H}) + D(\text{H,H})$	– 3.11	0.35	0.26
Gal: $D(\text{C,H}) + D(\text{H,H})$	– 3.41 ± 0.03/ – 3.45 ± 0.01	0.24 ± 0.03/0.25 ± 0.02	0.15 ± 0.00/0.13 ± 0.00
§Glc: $D(\text{C,H}) + D(\text{H,H})$	– 5.60	0.57	0.27
Glc: $D(\text{C,H}) + D(\text{H,H})$	– 5.59 ± 0.01/ – 5.64 ± 0.01	0.52 ± 0.00/0.49 ± 0.00	0.24 ± 0.00/0.23 ± 0.00
§Fru: $D(\text{C,H}) + D(\text{H,H})$	7.01	0.56	0.09
Fru: $D(\text{C,H}) + D(\text{H,H})$	– 6.26 ± 0.01/ – 6.29 ± 0.03	0.39 ± 0.01/0.46 ± 0.02	0.05 ± 0.00/0.04 ± 0.00
§Sacc: $D(\text{C,H})$	5.04	0.22	0.09
§Sacc: $D(\text{C,H})$	4.00	0.46	0.34
Sacc: $D(\text{C,H})$	3.48 ± 0.06/3.66 ± 0.09	0.28 ± 0.02/0.26 ± 0.03	0.35 ± 0.00/0.34 ± 0.00
§Sacc: $D(\text{C,H}) + D(\text{H,H})$	– 5.49	0.56	0.26
§Sacc: $D(\text{C,H}) + D(\text{H,H})$	– 4.99	0.47	0.48
Sacc: $D(\text{C,H}) + D(\text{H,H})$	– 4.92 ± 0.03/ – 5.08 ± 0.01	0.52 ± 0.00/0.52 ± 0.01	0.29 ± 0.00/0.25 ± 0.00
§Raff: $D(\text{C,H})$	3.87	0.57	0.42
Raff: $D(\text{C,H})$	5.63 ± 0.16/5.76 ± 0.11	0.32 ± 0.02/0.28 ± 0.00	0.25 ± 0.01/0.26 ± 0.01
§Raff: $D(\text{C,H}) + D(\text{H,H})$	– 3.87	0.40	0.54
Raff: $D(\text{C,H}) + D(\text{H,H})$	– 4.17 ± 0.03/ – 4.24 ± 0.02	0.58 ± 0.01/0.58 ± 0.02	0.36 ± 0.00/0.34 ± 0.00



Table 4.  $^{13}\text{C}$  Relaxation Rates for Raffinose. All measurements were performed twice to estimate the error of the relaxation rates.

	$T_1$ [ms]	r.m.s.d. $T_1$ [ms]	$T_2$ [ms]	r.m.s.d. $T_2$ [ms]	hetNOE
Gal C1	576	30	282	7	0.37
Gal C2	509	15	300	37	0.38
Gal C3	519	11	198	9	0.38
Gal C4	594	18	225	27	0.40
Gal C5	516	41	208	16	0.38
Avr. Gal	543		243		0.38
Glc C1	466	53	310	23	0.36
Glc C2	460	34	323	10	0.37
Glc C3	494	13	253	36	0.37
Glc C4	459	7	226	15	0.37
Glc C5	481	6	223	15	0.37
Avr. Glc	472		267		0.37
Fru C3	518	43	330	32	0.36
Fru C4	518	40	369	20	0.36
Fru C5	487	19	246	18	0.38
Avr. Fru	508		315		0.37
Gal C6	519	42	244	11	0.38
Glc C61	284	9	174	9	0.38
Glc C62	265	6	161	14	0.38
Fru C1	359	17	243	31	0.38
Fru C61	455	26	217	25	0.39
Fru C62	391	1	225	46	0.39

within 20%. However, for galactose we observe a reduction of the tensor size to *ca.* 60% compared to the other two tensors. We attribute this reduction to higher amplitude dynamics of the galactose moiety. This motion is reflected in  $T_1$ ,  $T_2$ , and in heteronuclear NOE data for the C-atoms (Table 4). An overall correlation time  $\tau_c$  of *ca.* 150 ps was calculated for raffinose. The average  $T_1$  values of galactose are larger than in glucose and fructose, indicating a larger amplitude for the mobility. The mobility is anisotropic since the two axial CH vectors at C1 and C4 in galactose show a higher mobility than the equatorial vectors. This finding would be in agreement with a rotation about the  $\varphi_1$  angle of the glycosidic linkage between galactose and glucose in raffinose (Fig. 4).

The structure calculations were performed on the basis of NOE distance information in addition to the dipolar couplings as given in Tables 1 and 2. For the calculation of the structure, the axial tensor component was changed from  $\pm 4.5$  to  $\pm 8.0$  Hz with a step size of 0.5 Hz, and the rhombicity was changed from 0.417 to 0.666 with a step size of 0.083 for the CHAPSO/DMPC dipolar couplings as described above (Materials and Methods) and based on the monosaccharide tensors. For  $D_{\text{ax}} = -4.50$  Hz,  $R = 0.667$  and  $D_{\text{ax}} = 4.50$  Hz,  $R = 0.583$ , the back-calculated values from the ten lowest-energy structures were  $D_{\text{ax}} = -4.17 \pm 0.02$  Hz,  $R = 0.58 \pm 0.01$  and  $D_{\text{ax}} = -4.24 \pm 0.01$  Hz,  $R = 0.58 \pm 0.02$ , respectively. For the second data set (written in brackets below), the change of sign of the axial component does not indicate strong differences of the tensor, which is obvious when comparing the  $x$ ,  $y$ , and  $z$  components of the initial tensor:  $D_{xx} = -0.57$  Hz,  $D_{yy} = -8.44$  Hz,  $D_{zz} = 9.00$  Hz to the final tensor:

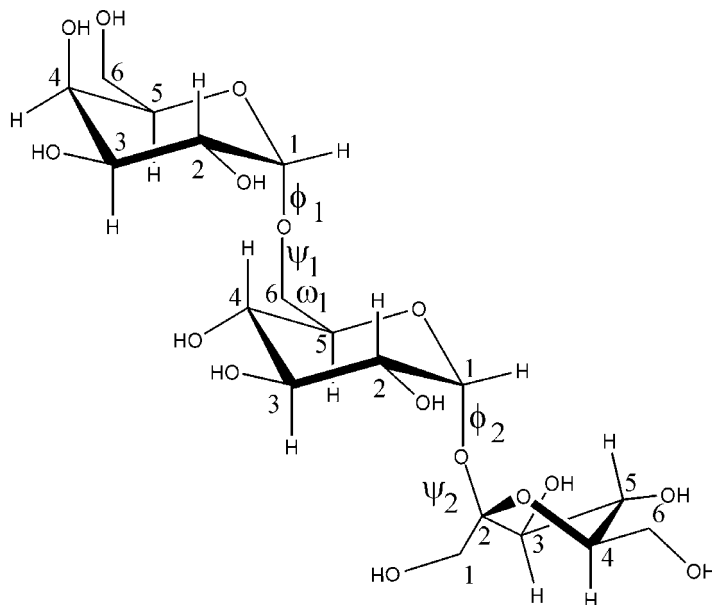


Fig. 4. Conformation of raffinose with the five rotatable dihedral angles as defined by  $\phi_1 = \text{Gal}(O5, C1, O1)\text{Glc}(C6)$ ,  $\psi_1 = \text{Gal}(C1, O1)\text{Glc}(C6, C5)$ ,  $\omega_1 = \text{Glc}(O6, C6, C5, O5)$ ,  $\phi_2 = \text{Glc}(O5, C1, O1)\text{Fru}(C2)$ ,  $\psi_2 = \text{Glc}(C1, O1)\text{Fru}(C2, O5)$

$D_{xx} = 0.54$  Hz,  $D_{yy} = 7.90$  Hz,  $D_{zz} = -8.47$  Hz (with  $D_{ax} = \frac{2D_{zz} - D_{yy} - D_{xx}}{6}$  and  $R = \frac{2(D_{xx} - D_{yy})}{3D_{zz}}$  and keeping in mind that the axis labels can be interchanged without changing the physics). The back-calculated monosaccharide alignment tensors for glucose and fructose agree quite well with the overall alignment tensor. The back-calculated galactose tensor remains smaller by *ca.* 60% than the two other ones.

Fig. 5 shows a stereoplot of the ten lowest-energy structures of raffinose calculated with the experimental data with  $D_{ax} = 4.50$  Hz and  $R = 0.583$  ( $Q = 0.34$ ). For the ten structures with lowest energies and lowest  $Q$  values, the glycosidic linkage between glucose and fructose is described by  $\phi_2 = 98.4 \pm 1.6^\circ$  ( $\phi_2 = 95.9 \pm 2.7^\circ$ ) and  $\psi_2 = -151.9 \pm 1.1^\circ$  ( $\psi_2 = -153.0 \pm 1.5^\circ$ ) (angles in braces describe the second tensor mentioned above). The glycosidic linkage between galactose and glucose is described by  $\phi_1 = 57.3 \pm 1.5^\circ$  ( $\phi_1 = 55.5 \pm 0.6^\circ$ ),  $\psi_1 = -178.3 \pm 0.7^\circ$  ( $\psi_1 = -176.8 \pm 0.6^\circ$ ) and  $\omega_1 = -62.8 \pm 0.5^\circ$  ( $\omega_1 = -62.4 \pm 0.5^\circ$ ) with a mean  $Q$  value of 0.36 (0.34). A recalculation of the glucose–fructose linkage ignoring the galactose experimental restraints did not change the result.

The result of the structure calculation did not change when further experimental restraints were taken into account. This is true for the interglycosidic NOE cross-peak (GlcH1/FruH1) that translates into a distance of 2.38 Å based on the GlcH1/H2 distance (2.41 Å in the neutron-diffraction structure of saccharose[43][44]) as a reference, as well as for the  $^3J(\text{H},\text{H})$  coupling constants between H3,H4 and H4,H5 protons in the fructose ring. These coupling constants were parameterized by means of

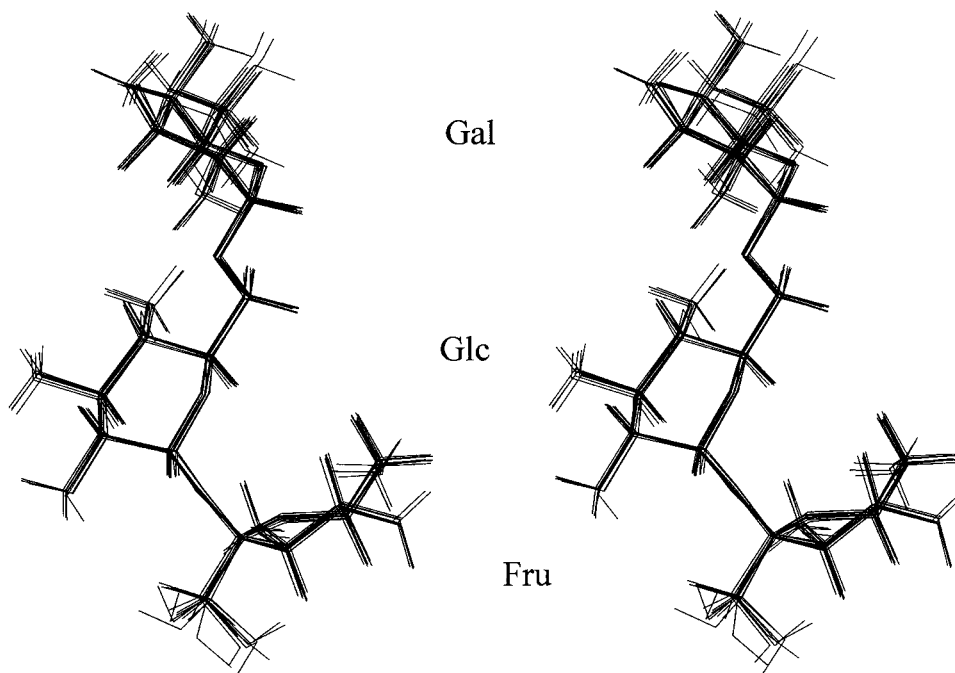


Fig. 5. Stereoplots of the 10 structures of raffinose with lowest energy as obtained from the dipolar, NOE, and J-coupling restraints. The glucose and galactose are in the chair conformation, the fructose in the  ${}^4T_3$  conformation. The r.m.s.d. of the structures is 0.28 Å (heavy atoms).

the *Karplus* curve of *Haasnoot et al.* [45][46]. Calculations with and without these coupling constants showed no difference and yielded the  ${}^4T_3$  conformation of the fructose ring.

The cross validation of the dipolar couplings is summarized in *Table 5*. The experimentally measured but so far unused dipolar couplings are reproduced quite well. Of special interest is the Fru-C6 H<sub>2</sub> group that has a distribution of conformations of 66% of  $g^+$  and 32% of  $g^-$  based on scalar coupling constants. Provided the correct structure of the trisaccharide was calculated, it should be possible to determine the

Table 5. Cross Validation of Raffinose Structure with Measured D(H,H) Dipolar Couplings, Which Were Not Used in the Structure Calculations. The two theoretical couplings are derived from the two optimal alignment tensors as described in the text. The errors are the standard deviations derived from the ten best NMR-derived structures of raffinose.

	Exper. [Hz]	Theory [Hz]
Fru-C6/H6	1.80	2.10/2.07
Fru-C6/H6'	-2.00	-1.78/ -1.66
Fru-H6/H6'	1.70	0.85/0.93
Gal-H1/Glc-H6'	± 1.82	-1.62 ± 0.06/ -1.60 ± 0.06
Gal-H5/Glc-H4	± 1.56	-1.66 ± 0.06/ -1.72 ± 0.07
Gal-H1/Glc-H6	± 1.45	0.81 ± 0.02/0.82 ± 0.03

distribution of populations based on the experimental dipolar couplings alone. Indeed, we calculate 62.5% of  $g^+$ , 32% of  $g^-$ , and 7.5% of  $t$  from the dipolar couplings (C6,H6', C6,H6, and H6',H6). Thus, it should be possible to predict the conformation also for those CH<sub>2</sub> groups where an analysis based on scalar coupling constants and NOEs was not possible. This is the case for the Fru-C1 H<sub>2</sub> and the Gal-C6 H<sub>2</sub> groups, for which the protons have identical chemical shifts and only the C,H dipolar couplings could be measured. From this sum of the dipolar couplings, we can calculate a range of populations for the staggered conformations. For Gal-C6 H<sub>2</sub>, the population-distributing parameterization is  $p(g^-) = 0.22 + 0.2x$ ;  $p(g^+) = 0.78(1 - x)$  and  $p(t) = 0.58x$  with  $x$  varying between 0 and 1. This prediction is in quite good agreement with the population distribution found for the C6 H<sub>2</sub> of galactose of  $p(g^-) = 21\%$ ,  $p(g^+) = 45\%$ ,  $p(t) = 25\%$  [47], in a study using selective deuteration in the C6 position of galactopyranose, if we set  $x = 0.406$ . According to the same analysis with dipolar couplings for the Fru-C1 H<sub>2</sub>, we find a population parameterization:  $p(g^-) = 0.29$ ;  $p(g^+) = 0.71(1 - x)$  and  $p(t) = 0.71x$  with  $x$  varying between 0 and 1.

Fitting of known substructures to the experimental dipolar couplings provides a measure for conformational similarity. Fitting the neutron-diffraction structure of saccharose [43][44] to the firm dipolar couplings for the saccharose part of raffinose yields a  $Q$  factor of 0.26, which is of the same size as  $Q$  factors obtained when fitting the dipolar couplings of the individual monosaccharides to an alignment tensor. Thus, it can be expected that the solution structure of the saccharose part in raffinose agrees well with the neutron-diffraction structure of saccharose. Indeed, the dihedral angles for the Glc-Fru linkage of  $\varphi_2 = 98.4 \pm 1.6^\circ$  ( $\varphi_2 = 95.9 \pm 2.7^\circ$ ) and  $\psi_2 = -151.9 \pm 1.1^\circ$  ( $\psi_2 = -153.0 \pm 1.5^\circ$ ) agree very well with the neutron-diffraction data ( $\varphi_2 = 107.8^\circ$  and  $\psi_2 = -159.8^\circ$ ). However, fitting the X-ray structure [42] of raffinose to the firm dipolar couplings yields a  $Q$  value of 0.54. This indicates that the solution structure of raffinose deviates from its X-ray structure. Indeed, the angles describing the Glc-Fru linkage  $\varphi_2 = 81.6^\circ$  and  $\psi_2 = -105.5^\circ$  deviate from the previously mentioned angles for the solution structure of raffinose.

**2.4. Structure Calculation of Saccharose.** The procedure used for raffinose was also used for the structure calculation of saccharose. Measured scalar and dipolar couplings are given in *Tables 6* and *7*. Dipolar couplings marked with a star in *Table 6* are again subject to conformational averaging or proton chemical-shift overlap and therefore not used for the refinement. The firm dipolar-coupling constants were fitted against the neutron-diffraction structure [43][44] of saccharose individually for each monosaccharide and for the whole structure [39]. The tensor sizes and rhombicities as well as the  $Q$  factors [40] are given in *Table 8* for hetero- and homonuclear dipolar couplings in combination ( $D(C,H) + D(H,H)$ ). Fitting of the dipolar couplings of glucose and fructose to the monosaccharide structure from the neutron-diffraction structure of saccharose yielded almost identical tensors ( $^6\text{Glc}$ :  $D(C,H) + D(H,H)$  and  $^6\text{Fru}$ :  $D(C,H) + D(H,H)$  in *Table 8*). Eight linearly independent vector orientations could be measured for glucose. Only five are available for fructose, which is the reason for  $Q = 0.0$ . Based on this result, for the structure calculation of saccharose, one tensor was assumed for the whole disaccharide. The axial tensor component ( $D_{\text{ax}}$ ) was varied from  $\pm 2.25$  to  $\pm 3.25$  Hz with a step size of 0.25 Hz and the rhombicity ( $R$ ) of the alignment tensor was changed from 0.325 to 0.625 with a step size of 0.05. For  $D_{\text{ax}} =$

Table 6. *Dipolar Couplings Determined for Saccharose in CHAPSO/DMPC (1/3.5; 7.5%)*. The couplings not marked by stars are the firm couplings as described in the text.

$D(\text{C,H})$ [Hz]		$D(\text{H,H})$ [Hz]	
Glc-C1/H1	1.95	Glc-H1/H2	-2.00
Glc-C2/H2	1.88	Glc-H2/H3	0.81
Glc-C3/H3	1.99	Glc-H3/H4	0.34
Glc-C4/H4	1.11	Glc-H4/H5	-0.45
Glc-C5/H5	1.80	Glc-H2/H4	0.00
*Glc-C6/H6	-0.88	Glc-H3/H5	0.00
*Fru-C1/H1	-1.25	Fru-H3/H4	-0.11
Fru-C3/H3	-3.31	Fru-H4/H5	-0.30
Fru-C4/H4	-2.73		
Fru-C5/H5	-4.49		
*Fru-C6-H6	-1.63		

Table 7. *Scalar Couplings Determined for Saccharose in Isotropic Solution*.

$^1J(\text{C,H})$ [Hz]		$^3J(\text{H,H})$ [Hz]	
Glc-C1/H1	169.6	Glc-H1/H2	4.02
Glc-C2/H2	144.3	Glc-H2/H3	10.07
Glc-C3/H3	145.4	Glc-H3/H4	9.13
Glc-C4/H4	144.8	Glc-H4/H5	9.94
Fru-C1/H1	289.4	Fru-H3/H4	8.77
Fru-C3/H3	144.8	Fru-H4/H5	8.45
Fru-C4/H4	144.6		
Fru-C5/H5	148.5		
Fru-C6/H6	287.6		

Table 8. *Tensor Sizes for Saccharose in CHAPSO/DMPC (1/3.5; 7.5%)*. The average alignment tensor and the standard deviation derived from the ten structures with lowest energy from 100 XPLOR calculations are given. The glucose and fructose structures are derived from the best solution structure of saccharose. The items indicated with \$ refer to the neutron diffraction structure of saccharose.

	$D_{\text{ax}}$ [Hz]	$R$	$Q$
$^{\text{\$}}\text{Glc: } D(\text{C,H}) + D(\text{H,H})$	-2.68	0.44	0.05
$\text{Glc: } D(\text{C,H}) + D(\text{H,H})$	$-2.58 \pm 0.46$	$0.46 \pm 0.01$	$0.07 \pm 0.01$
$^{\text{\$}}\text{Fru: } D(\text{C,H}) + D(\text{H,H})$	-2.32	0.61	0.00
$\text{Fru: } D(\text{C,H}) + D(\text{H,H})$	$-2.26 \pm 0.02$	$0.63 \pm 0.08$	$0.00 \pm 0.00$
$^{\text{\$}}\text{Sacc: } D(\text{C,H})$	3.19	0.65	0.06
$\text{Sacc: } D(\text{C,H})$	$-2.28 \pm 0.02$	$0.66 \pm 0.08$	$0.04 \pm 0.02$
$^{\text{\$}}\text{Sacc: } D(\text{C,H}) + D(\text{H,H})$	-2.74	0.37	0.16
$\text{Sacc: } D(\text{C,H}) + D(\text{H,H})$	$-2.51 \pm 0.02$	$0.43 \pm 0.02$	$0.09 \pm 0.01$

-2.50 Hz and  $R=0.425$ , the ten structures with the lowest energy have a  $Q$  value of 0.09. These structures have a self-consistent tensor with  $D_{\text{ax}} = -2.51$  Hz and  $R=0.43$  (Sacc:  $D(\text{C,H}) + D(\text{H,H})$  in Table 8). All other initial  $D_{\text{ax}}$  and  $R$  values were of lower self consistency. The back-calculated monosaccharide tensors agree well with the overall alignment tensor (Table 8). The ten structures with lowest energy not only have a low  $Q$  value of 0.09 but also a very small heavy-atoms r.m.s.d. value of 0.39 Å. The glycosidic linkage between glucose and fructose is described by  $\varphi = 99.7 \pm 3.8^\circ$  and  $\psi = -159.3 \pm 3.5^\circ$ . This is in excellent agreement with the neutron-diffraction structure of

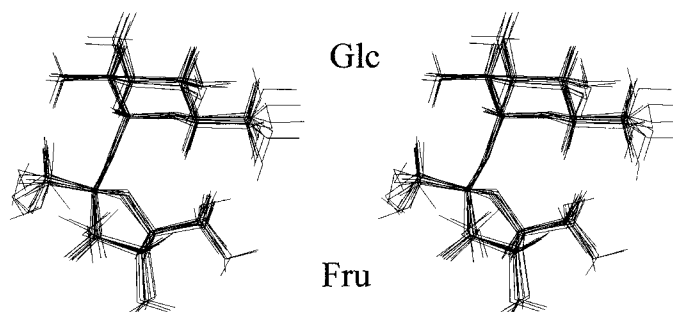


Fig. 6. Stereoview of the 10 structures of saccharose with lowest energy as obtained from the dipolar, NOE, and J-coupling restraints. The glucose is in the chair conformation, the fructose in the  ${}^4T_3$  conformation. The r.m.s.d. of the structures is 0.39 Å (heavy atoms).

saccharose:  $\varphi = 107.8^\circ$  and  $\psi = -159.8^\circ$ . The structure of saccharose is shown in Fig. 6 as a stereoplot.

The excellent agreement of the solution structure and neutron-diffraction structure of saccharose could be expected, because fitting of the firm experimentally determined dipolar couplings to the neutron-diffraction structure of saccharose yields a  $Q$  value of 0.16 ( ${}^8\text{Sacc}$ :  $D(\text{C,H}) + D(\text{H,H})$  in Table 8). This is almost as small as the  $Q$  values obtained for the individual monosaccharides in saccharose. Therefore, the solution structure of saccharose is expected to be highly similar to its neutron-diffraction structure.

The  $\text{CH}_2$  groups were left out from the analysis because of overlap or conformational averaging. However, with the known tensor size the distribution of conformations for the  $\text{CH}_2$  groups can be obtained like in raffinose. We find for the glucose  $\text{C6H}_2$  group:  $p(g^-) = 0.61x$ ;  $p(g^+) = 0.30 + 0.09x$  and  $p(t) = 0.78(1 - x)$  with  $x$  varying between 0 and 1. Again, this parameterization corresponds well with the exact values determined from selectively deuterated carbohydrates [48] ( $p(g^-) = 57\%$ ,  $p(g^+) = 38\%$ ,  $p(t) = 5\%$ ), resulting in an  $x$  value of 0.935. The following conformational population was found for fructose:  $\text{C1H}_2$ :  $p(g^-) = 0.31$ ;  $p(g^+) = 0.69(1 - x)$  and  $p(t) = 0.69x$  with  $x$  varying between 0 and 1;  $\text{C6H}_2$ :  $p(g^-) = 0.37x$ ;  $p(g^+) = 0.2 + 0.16x$  and  $p(t) = 0.80(1 - x)$ .

**3. Conclusion.** – We have shown that it is possible to measure  $D(\text{H,H})$  in addition to  $D(\text{C,H})$  dipolar coupling constants in sugars with the E.COSY method. From both types of dipolar-couplings, it is possible to determine a well-defined alignment tensor for the individual monosaccharides and check for differential monosaccharide mobility. Monosaccharide  $Q$  values are a good measure to check whether the solution structure agrees with structural models of oligosaccharides derived from modeling or crystal structures. Inclusion of the H,H dipolar couplings quite dramatically increases the precision of carbohydrate structures compared to those derived from NOE and  $J$  coupling constants alone. This is reflected in the sharp decrease of the r.m.s.d. values of the heavy atoms of the raffinose structures based on only NOE and  $J$  coupling data: r.m.s.d. = 1.02 Å, and when using a combination of NOE,  $J$  couplings, and hetero- and homonuclear dipolar couplings: r.m.s.d. = 0.28 Å. In principle, four symmetry-related

orientations of the monosaccharides are possible. However, due to the short linkers between the monosaccharides only one of these orientations was found in this work [9]. Therefore, one alignment was sufficient to fully define the entire conformation. Differential dynamic behavior was clearly observed for the galactose moiety, which had a significantly reduced alignment tensor when compared to those of the other monosaccharides. Therefore, further refinement of the model is expected when the full dynamic information of the monosaccharide moieties are taken into account.

The *Fonds der Chemischen Industrie*, the *DFG* and the *MPG* supported this work. *J. M.* and *W. P.* are supported by a *Kekulé* stipend of the *Fonds der Chemischen Industrie*. We are grateful to *Klaus M. Fiebig* (*MRPharm*, Frankfurt, Germany) for discussions of the manuscript. We would like to acknowledge discussions with *Thomas Peters* (University of Lübeck, Germany), *James H. Prestegard* (CCRC, University of Georgia, USA) for making a copy of a manuscript describing related work on other oligosaccharides available prior to publication, and *Steven W. Homans* (University of Leeds, UK) for making available his carbohydrate-optimized force field that we used in all structure calculations. All measurements were done at the *Large Scale Facility* for Biomolecular NMR at the University of Frankfurt. We would like to thank *Michael Bolte* (University of Frankfurt, Germany) for help with the *CCDC* files.

## REFERENCES

- [1] J. R. Tolman, J. M. Flanagan, M. A. Kennedy, J. H. Prestegard, *Proc. Natl. Acad. Sci. U.S.A.* **1995**, 92, 9279.
- [2] N. Tjandra, A. Bax, *Science* **1997**, 278, 1111.
- [3] C. A. Bewley, K. R. Gustafson, M. R. Boyd, D. G. Covell, A. Bax, G. M. Clore, A. M. Gronenborn, *Nat. Struct. Biol.* **1998**, 5, 571.
- [4] M. Cai, Y. Huang, R. Zheng, S.-Q. Wei, R. Ghirlando, M. S. Lee, R. Craigie, A. M. Gronenborn, G. M. Clore, *Nat. Struct. Biol.* **1998**, 5, 903.
- [5] G. M. Clore, M. R. Straich, C. A. Bewley, M. Cai, J. Kuszewski, *J. Am. Chem. Soc.* **1999**, 121, 6513.
- [6] D. Yang, J. R. Tolman, N. K. Goto, L. E. Kay, *J. Biomol. NMR* **1998**, 12, 325.
- [7] D. W. Yang, R. A. Venters, G. A. Mueller, W. Y. Choy, L. E. Kay, *J. Biomol. NMR* **1999**, 14, 333.
- [8] P. Permi, A. Annala, *J. Biomol. NMR* **2000**, 16, 221.
- [9] H. M. Al-Hashimi, P. J. Bolon, J. H. Prestegard, *J. Magn. Reson.* **2000**, 142, 153.
- [10] P. J. Bolon, H. M. Al-Hashimi, J. H. Prestegard, *J. Mol. Biol.* **1999**, 293, 107.
- [11] E. T. Olejniczak, R. P. Meadows, H. Wang, M. Cai, D. G. Nettlesheim, S. W. Fesik, *J. Am. Chem. Soc.* **1999**, 121, 9249.
- [12] H. v. Halbeek, *Curr. Opin. Struct. Biol.* **1994**, 4, 697.
- [13] G. R. Kiddle, S. W. Homans, *FEBS Lett.* **1998**, 436, 128.
- [14] C. Landersjö, C. Hoog, A. Maliniak, G. Widmalm, *J. Phys. Chem. B* **2000**, 104, 5618.
- [15] M. Martin-Pastor, A. C. Bush, *Biochemistry* **2000**, 39, 4674.
- [16] M. Martin-Pastor, A. C. Bush, *Carbohydr. Res.* **2000**, 323, 147.
- [17] T. Rundlöf, C. Landersjö, K. Lycknert, A. Maliniak, G. Widmalm, *Magn. Reson. Chem.* **1998**, 36, 773.
- [18] M. G. Clore, A. Gronenborn, A. Bax, *J. Magn. Reson.* **1998**, 133, 216.
- [19] G. Bodenhausen, D. J. Ruben, *Chem. Phys. Lett.* **1980**, 69, 185.
- [20] T. Carlomagno, W. Peti, C. Griesinger, *J. Biomol. NMR* **2000**, 17, 99.
- [21] C. Griesinger, O. W. Sørensen, R. R. Ernst, *J. Am. Chem. Soc.* **1985**, 107, 6394.
- [22] C. Griesinger, O. W. Sørensen, R. R. Ernst, *J. Chem. Phys.* **1986**, 85, 6837.
- [23] C. Griesinger, O. W. Sørensen, R. R. Ernst, *J. Magn. Reson.* **1987**, 75, 474.
- [24] W. Peti, C. Griesinger, *J. Am. Chem. Soc.* **2000**, 122, 3975.
- [25] B. E. Ramirez, A. Bax, *J. Am. Chem. Soc.* **1998**, 120, 9106.
- [26] H. Oschkinat, J. Freeman, *J. Magn. Reson.* **1984**, 60, 164.
- [27] H. Kessler, A. Müller, H. Oschkinat, *Magn. Reson. Chem.* **1985**, 23, 844.
- [28] H. Kessler, H. Oschkinat, *Angew. Chem.* **1985**, 97, 689.
- [29] C. R. Sanders, J. P. Schwonek, *Biochemistry* **1992**, 31, 8898.
- [30] H. Wang, M. Eberstadt, T. Olejniczak, R. P. Meadows, S. W. Fesik, *J. Biomol. NMR* **1998**, 12, 443.
- [31] M. Ottiger, A. Bax, *J. Biomol. NMR* **1998**, 12, 361.

- [32] W. Peti, C. Griesinger, *J. Am. Chem. Soc.* **2000**, *122*, 3975.
- [33] L. Mueller, *J. Magn. Reson.* **1987**, *72*, 191.
- [34] S. Macura, Y. Huang, D. Suter, R. R. Ernst, *J. Magn. Reson.* **1981**, *43*, 259.
- [35] S. Macura, K. Wüthrich, R. R. Ernst, *J. Magn. Reson.* **1982**, *46*, 269.
- [36] A. T. Bruenger, Yale University Press, New Haven, 1992.
- [37] S. W. Homans, *Biochemistry* **1990**, *29*, 9110.
- [38] J. Meiler, N. Blomberg, M. Nilges, C. Griesinger, *J. Biomol. NMR* **2000**, *16*, 245.
- [39] J. Meiler, W. Peti, C. Griesinger, *J. Biomol. NMR* **2000**, *17*, 283.
- [40] G. Cornilescu, J. L. Marquardt, M. Ottiger, A. Bax, *J. Am. Chem. Soc.* **1999**, *120*, 6836.
- [41] Y. Nishida, H. Hiroshi, H. Ohru, H. Meguro, J. Uzawa, D. Reimer, V. Sinnwell, H. Paulsen, *Tetrahedron Lett.* **1988**, *29*, 4461.
- [42] G. A. Jeffrey, D. B. Huang, *Carbohydr. Res.* **1990**, *206*, 173.
- [43] G. M. Brown, H. A. Levy, *Science* **1963**, *141*, 921.
- [44] G. M. Brown, H. A. Levy, *Acta Crystallogr., Ser. B.* **1973**, *29*, 790.
- [45] C. A. G. Haasnoot, F. A. A. M. Leeuw, C. Altona, *Tetrahedron* **1980**, *36*, 2783.
- [46] C. A. G. Haasnoot, F. A. A. M. Leeuw, H. P. M. de Leeuw, C. Altona, *Org. Magn. Reson.* **1981**, *15*, 43.
- [47] H. Ohru, Y. Nishida, H. Higuchi, H. Hori, H. Meguro, *Can. J. Chem.* **1987**, *65*, 1145.
- [48] Y. Nishida, H. Ohru, H. Meguro, *Tetrahedron Lett.* **1984**, *25*, 1575.

Received December 21, 2000